Realization of Single-Qubit Positive-Operator-Valued Measurement via a One-Dimensional Photonic Quantum Walk

Zhihao Bian,[1] Jian Li,[1] Hao Qin,[1] Xiang Zhan,[1] Rong Zhang,[1] Barry C. Sanders,[2,3,4,5] and Peng Xue[1,6,7,*]
[1]Department of Physics, Southeast University, Nanjing 211189, China
[2]Hefei National Laboratory for Physical Sciences at Microscale and Department of Modern Physics, University of Science and Technology of China, Hefei, Anhui 230026, China
[3]Shanghai Branch, CAS Center for Excellence and Synergetic Innovation Center in Quantum Information and Quantum Physics, University of Science and Technology of China, Shanghai 201315, China
[4]Institute for Quantum Science and Technology, University of Calgary, Alberta T2N 1N4, Canada
[5]Program in Quantum Information Science, Canadian Institute for Advanced Research, Toronto, Ontario M5G 1Z8, Canada
[6]State Key Laboratory of Precision Spectroscopy, East China Normal University, Shanghai 200062, China
[7]Beijing Institute of Mechanical and Electrical Space, Beijing 100094, China
(Received 15 January 2015; published 22 May 2015)

We perform generalized measurements of a qubit by realizing the qubit as a coin in a photonic quantum walk and subjecting the walker to projective measurements. Our experimental technique can be used to realize, photonically, any rank-1 single-qubit positive-operator-valued measure via constructing an appropriate interferometric quantum-walk network and then projectively measuring the walker's position at the final step.

DOI: 10.1103/PhysRevLett.114.203602 PACS numbers: 42.50.Ex, 03.67.Ac, 03.67.Lx, 42.50.Dv

Quantum walks (QWs) exhibit distinct features compared to classical random walks with applications to quantum algorithms [1,2]. The one-dimensional (1D) discrete-time QW is a process in which the evolution of a quantum particle on a 1D lattice depends on the state of a coin, typically a two-level system, or qubit. Controlling the coin degree of freedom indirectly controls the walker, and, through this indirect control, the walker's state can be measured to infer the coin state. Rigorously speaking, walker-coin entanglement and projective measurement of the walker yields a positive-operator-valued measure (POVM) on a single qubit [3]. Furthermore, any rank-1 or rank-2 single-qubit POVM can be generated by a judiciously engineered QW. The QW model is capable of serving as a universal quantum computer [4–6] as well as replicating quantum transport processes [7,8], so an important question is how far the QW model can be pushed towards replacing other quantum information tasks such as generalized measurements [9], which we address here experimentally. We demonstrate, experimentally, the capability of performing such generalized measurements of a qubit by realizing the walker in the path degree of freedom of a photon and the coin state as polarization and performing optical interferometry with a path-based photodetector to perform a POVM on the photon's polarization state.

A POVM [9] is a set of positive operators E_i such that the probability of obtaining the ith outcome is given by $\mathrm{Tr}(E_i\rho)$, where ρ is the density operator for the system being measured. A POVM must satisfy the completeness condition, $\sum_i E_i = 1$, which is equivalent to saying the probabilities of the outcomes must sum to unity. Realizing a POVM is important as a POVM is needed for generalized acquisition of information thereby associated with a multitude of quantum information tasks such as quantum state estimation and tomography [10], quantum cloning [11], entanglement distillation [12], and generalized quantum cryptography protocols [13]. Single-qubit POVMs have been performed experimentally in photonic systems via polarization-based free-space interferometers [14–17]. POVMs' wide applications include unambiguous state discrimination [18–21] and quantum state tomography in terms of symmetric informationally complete (SIC) POVMs [22–25]. For the former case, unambiguous state discrimination between N states has $N+1$ outcomes: the N possible conclusive results, and the inconclusive result. As no projective measurement in an N-dimensional Hilbert space can have more than N outcomes, generalized measurements such as POVMs are required, whereas a SIC POVM is a generalized measurement on a N-dimensional quantum state, which consists of N^2 subnormalized projection operators with equal pairwise fidelity.

Our goal is to realize, experimentally, a single-qubit POVM and to discriminate between nonorthogonal initial coin states via executing a properly engineered QW whose projective walker measurement is sometimes inconclusive [3]. To achieve a site-specific POVM, we control the internal degree of freedom of the measured two-level coin. Here, we report our successful experimental realization of POVMs, including the unambiguous state discrimination of two equally probable single-qubit states and a single-qubit SIC POVM, via a one-dimensional photonic QW.

We focus on rank-1 POVMs, as higher-rank POVMs can be constructed as a convex combination of rank-1 elements [3]. Our experimental technique can be used to realize,

photonically, any rank-1 single-qubit POVM via constructing an interferometric QW and projectively measuring the walker's position at the final step.

A standard model of a 1D discrete-time QW consists of a walker carrying a coin that is flipped before each step. In the coin-state basis $\{|0\rangle, |1\rangle\}$, the site-dependent coin rotation for the nth step $C_{x,n} \in SU(2)$ is applied to the coin when the walker in the position x, followed by a conditional position shift due to the outcome of the coin flipping for each step $T = \sum_x |x+1\rangle\langle x| \otimes |0\rangle\langle 0| + |x-1\rangle\langle x| \otimes |1\rangle\langle 1|$. The unitary operation for the nth step is $U_n = T \sum_x |x\rangle\langle x| \otimes C_{x,n}$.

We commence with the simplest nontrivial case, namely, a three-step QW approach to implement an unambiguous state discrimination of two single-qubit states. Two nonorthogonal pure states can always be encoded as

$$|\phi^{\pm}\rangle = \cos\frac{\phi}{2}|0\rangle \pm \sin\frac{\phi}{2}|1\rangle, \tag{1}$$

where $\phi \in [0, \pi/2]$. Our objective is to discriminate these two states with equal prior probability for three outcomes: conclusively measuring one or the other state (1) or obtaining an inconclusive measurement result. We prepare an initial coin state in either of the two states (1). For a properly engineered QW procedure, the walker with the different initial coin states arrives at different position distributions. By projective measurement onto the walker's position, initial coin states can be discriminated.

For our realization, the coin is initially prepared in $|\phi^{\pm}\rangle$, and the walker starts from the origin $|x = 0\rangle$. The site-dependent coin rotations for the first three steps are

$$C_{1,2} = \begin{pmatrix} \sqrt{1-\tan^2\frac{\phi}{2}} & \tan\frac{\phi}{2} \\ \tan\frac{\phi}{2} & -\sqrt{1-\tan^2\frac{\phi}{2}} \end{pmatrix},$$
$$C_{-1,2} = \sigma_x = \begin{pmatrix} 0 & 1 \\ 1 & 0 \end{pmatrix}, \quad C_{0,3} = \frac{1}{\sqrt{2}}\begin{pmatrix} 1 & 1 \\ 1 & -1 \end{pmatrix}, \tag{2}$$

and $\mathbb{1}$ elsewhere, for example $C_{0,1} = \mathbb{1}$. Each step, the site-dependent coin rotations are followed by a conditional position shift T. Then, the initial walker-coin states $|\varphi_0^{\pm}\rangle = |0\rangle|\phi^{\pm}\rangle$ evolve into

$$|\varphi_3^{+}\rangle = \sqrt{\cos\phi}|3\rangle|0\rangle + \sqrt{2}\sin\frac{\phi}{2}|1\rangle|0\rangle,$$
$$|\varphi_3^{-}\rangle = \sqrt{\cos\phi}|3\rangle|0\rangle - \sqrt{2}\sin\frac{\phi}{2}|-1\rangle|1\rangle, \tag{3}$$

respectively. The walker is projectively measured in the position basis. If the position measurement outcome is $x = 1$ ($x = -1$), then, we ascertain that the initial coin state was $|\phi^{+}\rangle$ ($|\phi^{-}\rangle$). If the walker is, instead, measured in $x = 3$, we do not know the initial coin state; that is, $x = 3$ corresponds to an inconclusive result with probability $\eta_{\mathrm{err}} = |\langle\phi_+|\phi_-\rangle| = \cos\phi$. The probability of the inclusive result depends on the similarity of the two states, which agrees with the Ivanovic-Dieks-Peres bound obtained from the optimum strategy of this kind for unambiguous state discrimination [18–20]. For the boundary case of $\phi = 0$, the two states in Eq. (1) are the same, whereas, for the case of $\phi = \pi/2$, the two states are orthogonal and the measurement is projective.

The QW is proven to be universal for generating an arbitrary single-qubit POVM [3], and we show an example of a properly engineered five-step QW for generating a single-qubit SIC POVM. For example, we choose

$$|\xi^1\rangle = |0\rangle, \quad |\xi^2\rangle = \frac{1}{\sqrt{3}}(|0\rangle + \sqrt{2}|1\rangle),$$
$$|\xi^3\rangle = \frac{1}{\sqrt{3}}(|0\rangle + \lambda\sqrt{2}|1\rangle), \quad |\xi^4\rangle = \frac{1}{\sqrt{3}}(|0\rangle + \lambda^*\sqrt{2}|1\rangle), \tag{4}$$

satisfying $|\langle\xi^i|\xi^j\rangle| = 3^{-1/2}$ for $i \neq j$ and $\frac{1}{2}\sum_i^4 |\xi^i\rangle\langle\xi^i| = \mathbb{1}$ for $\lambda = e^{i2\pi/3}$. Now, we construct four states orthogonal to the above states (4) and prepare the coin state in one of these four coin states

$$|\psi^1\rangle = |1\rangle, \quad |\psi^2\rangle = \frac{1}{\sqrt{3}}(\sqrt{2}|0\rangle - |1\rangle),$$
$$|\psi^3\rangle = \frac{1}{\sqrt{3}}(\sqrt{2}|0\rangle - \lambda|1\rangle),$$
$$|\psi^4\rangle = \frac{1}{\sqrt{3}}(\sqrt{2}|0\rangle - \lambda^*|1\rangle). \tag{5}$$

The site-dependent coin rotations for the first five steps are

$$C_{1,2} = \frac{1}{\sqrt{2}}\begin{pmatrix} 1 & -1 \\ -1 & -1 \end{pmatrix}, \quad C_{0,3} = \frac{1}{\sqrt{2}}\begin{pmatrix} -1 & 1 \\ 1 & 1 \end{pmatrix},$$
$$C_{-1,2} = C_{-1,4} = \sigma_x,$$
$$C_{1,4} = \frac{1}{\sqrt{3}}\begin{pmatrix} \sqrt{2} & 1 \\ 1 & -\sqrt{2} \end{pmatrix},$$
$$C_{0,5} = \frac{1}{\sqrt{2}}\begin{pmatrix} e^{-i(\pi/3)} & e^{i(\pi/6)} \\ e^{i(\pi/3)} & e^{-i(\pi/6)} \end{pmatrix}, \tag{6}$$

and $\mathbb{1}$ elsewhere. The coin operators chosen here depend only on the states we aim to discriminate. Following the five-step QW procedure including specific site-dependence coin rotations, the initial states of the walker-coin system $|\varphi_0^i\rangle = |0\rangle|\psi^i\rangle$ $(i = 1, 2, 3, 4)$ evolve to

$$|\varphi_5^1\rangle = \frac{1}{\sqrt{3}}(-|3\rangle|0\rangle - i|1\rangle|0\rangle + i|-1\rangle|1\rangle),$$
$$|\varphi_5^2\rangle = \frac{1}{\sqrt{3}}(|5\rangle|0\rangle - e^{-i(\pi/3)}|1\rangle|0\rangle - e^{i(\pi/3)}|-1\rangle|1\rangle),$$
$$|\varphi_5^3\rangle = \frac{1}{\sqrt{3}}(|5\rangle|0\rangle - e^{-i(\pi/6)}|3\rangle|0\rangle - |1\rangle|0\rangle),$$
$$|\varphi_5^4\rangle = \frac{1}{\sqrt{3}}(|5\rangle|0\rangle - e^{i(\pi/6)}|3\rangle|0\rangle - |-1\rangle|1\rangle). \quad (7)$$

Evidently, the final walker-coin states have differing support over position x, so by measuring the position of the walker, the initial coin state can be determined with some degree of certainty. Specifically, $|\varphi_5^{1,2,3,4}\rangle$ cannot be found at $x = 5$, $x = 3$, $x = -1$, and $x = 1$, respectively. Thus, we realize all elements $|\xi^i\rangle\langle\xi^i|/2$ $(i = 1, 2, 3, 4)$ of a qubit SIC POVM through a QW procedure.

The realization of the unambiguous state discrimination of two equally probable single-qubit states via a three-step QW is shown in Fig. 1(a). Inspired by [26,27] but, instead, realizing site-dependent coin operations with unmounted fixed-angle wave plates (WPs) calibrated prior to insertion by tomography rather than rotatable WPs, we can

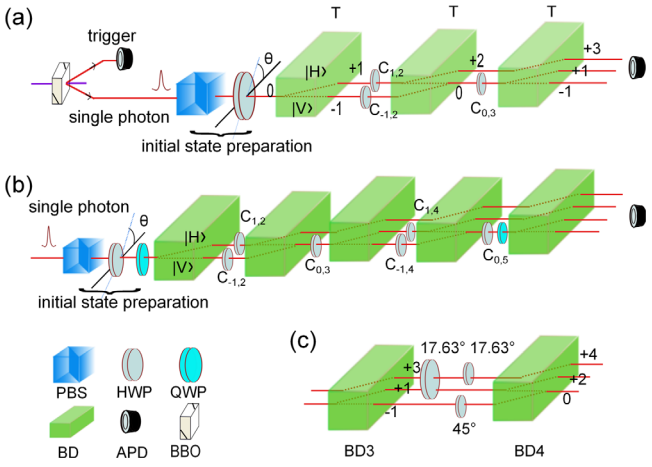

FIG. 1 (color online). Experimental schematic. (a) Detailed sketch of the setup for realization of unambiguous state discrimination of two equally probable single-qubit states via a three-step QW. Single photons are created via SPDC in a BBO crystal. One photon in the pair is detected to herald the other photon, which is injected into the optical network. (b) Setup for realization of a qubit SIC POVM via a five-step QW. The initial coin states for realization of SIC POVM $|\psi^{1,2}\rangle$ are prepared by a HWP, whereas $|\psi^{3,4}\rangle$ are prepared by a QWP with certain setting angles. Site-dependent coin flipping is realized by HWPs (and QWPs) with different setting angles placed in different optical modes. (c) Detailed interferometric setup formed by the third and fourth BDs, which are used in the experimental realization of a qubit SIC POVM. Unmounted WPs are inserted into specific optical paths such that only certain beams transit. WP angles are fixed (not rotatable) and calibrated via tomography before insertion.

demonstrate POVMs. The coin qubit is encoded in the horizontal $|H\rangle = |0\rangle$ and vertical polarization $|V\rangle = |1\rangle$ of photons. The walker's positions are represented by longitudinal spatial modes. The polarization degenerate photon pairs are generated via type-I spontaneous parametric down conversion (SPDC) in 0.5 mm-thick nonlinear-β-barium-borate (BBO) crystal, which is pumped by a cw diode laser with 90 mW of power. For 1D QWs, triggering on one photon prepares the other beam at wavelength 801.6 nm into a single-photon state. Total coincidence counts are about 3.4×10^4 over a collection time of 60 s, and the probability of randomly creating more than one simultaneous photon pair is, thus, less than a negligible 10^{-4}.

The initial coin state can be prepared by the half-wave plate (HWP) or quarter-wave plate (QWP) right after the polarizing beam splitter (PBS) shown in Fig. 1. After passing through the PBS and WP, the down-converted photons are steered into the optical modes of the linear-optical network formed by a series of birefringent calcite beam displacers (BDs) and WPs. The site-dependent coin rotations $C_{x,n}$ for the nth step can be realized by HWPs and QWPs with specific setting angles placed in mode x.

The conditional position shift is implemented by a BD with length 28 mm and clear aperture 10×10 mm. The optical axis of each BD is cut so that vertically polarized photons are directly transmitted and horizontal photons move up a 2.7 mm lateral displacement into a neighboring mode and interfere with the vertical photons in the same mode. Certain pairs of BDs form an interferometer and are placed in sequence and need to have their optical axes mutually aligned.

We attain interference visibility of 0.992 for each step. Output photons are detected using avalanche photo-diodes (APDs) (7 ns time window) with a dark-count rate of less than 100 s^{-1} whose coincidence signals, monitored using commercially available counting logic, are used to post-select two single-photon events. The walker position probabilities are obtained by normalizing the coincidence counts on each mode with respect to the total count for each respective step.

For site-dependent coin flipping, the optical delay usually needs to be considered. Fortunately, in our experiment on unambiguous state discrimination, only the first and second BDs form an interferometer. For the third step of the QW, the photons in mode $x = 2$, which are all in $|H\rangle$, move up to mode $x = 3$ after the last BD and, thus, do not interfere with other photons. Thus, no optical compensate is needed and the difficulty of the realization of the experiment is decreased.

The measured probability distributions of a three-step QW for unambiguous state discrimination are shown in Fig. 2. We choose a different coefficient ϕ and prepare the initial coin state to the corresponding state $|\phi^{\pm}\rangle$. For either of the two states, the photons undergoing the QW network are measured at the mode $x = 3$ for inclusive results and

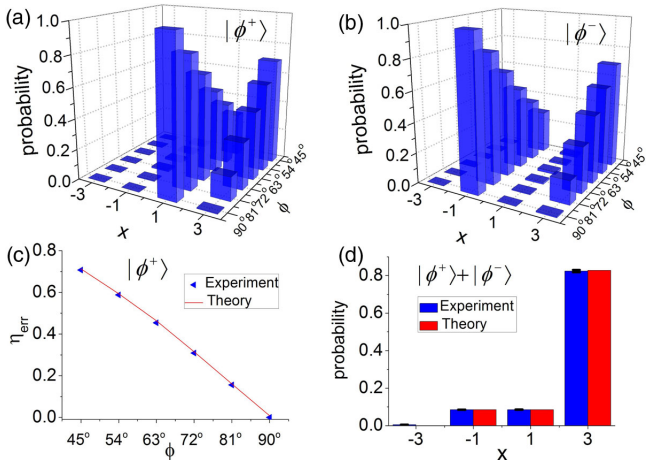

FIG. 2 (color online). Experimental data for unambiguous state discrimination via a photonic QW. Measured position distributions for the three-step QW with site-dependent coin and (a) initial coin state $|\phi^+\rangle$ and (b) $|\phi^-\rangle$; various coefficients ϕ of $|\phi^\pm\rangle$ for unambiguous state discrimination. (c) Measured probability η_{err} for inconclusive results vs parameters ϕ, which are related to the state to be discriminated; compared to theoretical predictions. Error bars are smaller than portrayed by the symbols. (d) Position distribution for the three-step QW with initial coin state $|H\rangle$, which is an equally weighted superposition of $|\phi^\pm\rangle$ with $\phi = 45°$. The blue and red bars show the experimental data and theoretical predictions, respectively. Error bars indicate the statistical uncertainty.

$x = \pm 1$ for conclusive results. Two pronounced peaks for each ϕ shown in the probability distribution in Figs. 2(a) and 2(b) validate the demonstration of unambiguous state discrimination. With ϕ increasing from 45° to 90°, the probability of inconclusive results η_{err} of the discrimination of the state $|\phi^+\rangle$ decreases from 0.7139 ± 0.0030 to 0.0070 ± 0.0060 (from 0.7125 ± 0.0031 to 0.0080 ± 0.0071 to discriminate the state $|\phi^-\rangle$) shown in Fig. 2(c), agreeing with the Ivanovic-Dieks-Peres bound.

Taking a superposition of $|\phi^\pm\rangle$ as an initial coin state $a|\phi^+\rangle + b|\phi^-\rangle$ (non-normalized), with $a, b \in \mathbb{R}$, the ratio of the probabilities for the two conclusive results is a^2/b^2, which is also demonstrated in our experiment. In Fig. 2(d), we show with $a = b$ the probabilities of $x = 1$ and $x = -1$ are measured approximately equal, i.e., $P(1) = 0.0854 \pm 0.0015$ and $P(-1) = 0.0850 \pm 0.0015$.

We characterize experimental performance by the one-norm distance [26] between the walker distribution obtained experimentally $P^{\mathrm{exp}}(x)$ vs theoretically $P^{\mathrm{th}}(x)$ over integer-valued position x. This distance is

$$d = \frac{1}{2}\sum_x |P^{\mathrm{exp}}(x) - P^{\mathrm{th}}(x)|, \tag{8}$$

and a small distance indicates a successful experimental realization.

The unambiguous state discrimination is confirmed by direct measurement and found to be consistent with the ideal theoretical values at the level of the small average distance $d < 0.02$ and the fidelity of the coin state measured in the position ($x = \pm 1$) $F > 0.9911$.

The realization of a qubit SIC POVM via a properly engineered five-step QW is shown in Fig. 1(b). For site-dependent coin flipping, the challenge is placing the WP into a given optical mode without influencing the photons in the other modes. For example, in Fig. 1(c), for the fourth step, the polarizations of photons in modes $x = \pm 1$ should be rotated by a HWP with setting angles $\theta_H = 17.63°$ and $\theta_H = 45°$, respectively, to realize the site-dependent coin rotations $C_{\pm 1,4}$, and the photons in those two modes interfere in mode $x = 0$ at the fourth BD. Because of the small separations between the neighboring modes, it is difficult to inset a HWP in the middle mode $x = 1$ and avoid the photons in the neighboring modes passing through it.

In our experiment, we place a HWP with $\theta_H = 17.63°$ in both modes $x = 1$ and $x = 3$ followed by a HWP with the same angle in mode $x = 3$ and a HWP with 45° in mode $x = -1$. Thus, the photons in modes $x = \pm 1$ do not suffer an optical delay and interfere with each other with a high visibility. The polarizations of photons in mode $x = 3$ are not changed after two HWPs with the same angle. The photons in mode $x = 3$ do not interfere with those in the other modes, though there is optical delay between them. Hence, optical compensation is not required.

The measured probability distributions of a five-step QW for a qubit SIC POVM are shown in Fig. 3, which agree well with the theoretical predictions. Using the experimental distribution of the QW with the initial coin state $|\psi^1\rangle$ as an example, after five steps, the probability $P(5)$ is

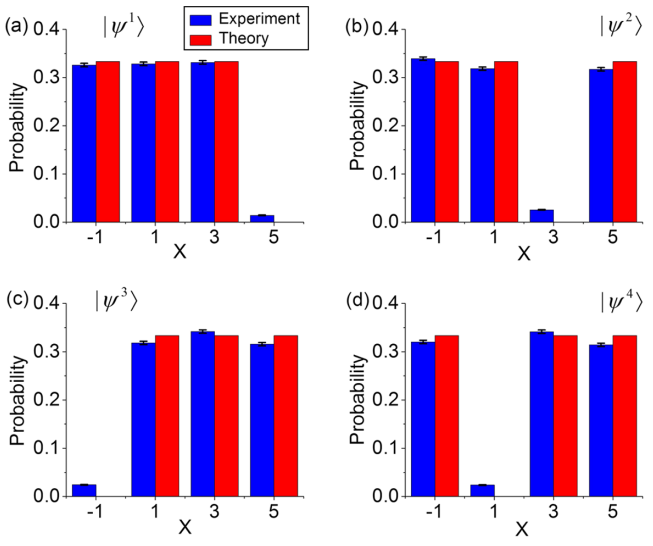

FIG. 3 (color online). Experimental data of a qubit SIC POVM via a photonic QW. Measured probability distributions of the five-step QW with the site-dependent coin rotations and four different initial coin states $|\psi^i\rangle$ with $i = 1, 2, 3, 4$ in (a)–(d), respectively.

measured as 0.0140 ± 0.0007 and, thus, is very small compared to the probabilities of the photons being measured in the other modes, i.e., $P(-1) = 0.3260 \pm 0.0036$, $P(1) = 0.3285 \pm 0.0037$, $P(3) = 0.3315 \pm 0.0037$, which ensures that one of the elements of a qubit SIC POVM is realized successfully. The small distance $d < 0.033$ demonstrates strong agreement between theoretical and measured distribution after five steps. Dominant sources of experimental errors are an inaccuracy of angles controlled by the WPs and imperfect nonunit visibility.

We report three figures of merit to characterize aspects of our experiment: interference visibility whose value conveys primarily how parallel the BDs are but is also affected by all other imperfections; polarization fidelity affected mostly by the quality of the WP placement; and one-norm distance to convey how well the task itself is performed. In the Supplemental Material [28], we add a fourth figure of merit, namely, fidelity of the reconstructed density matrix as background information for specialists on the reliability of the inference of the coin state.

In summary, we experimentally show that QWs are capable of performing generalized measurements on a single qubit. Our demonstration employs a novel photonic QW with site-dependent coin rotation for realizing a generalized measurement [3]. The key experimental advance for realizing a QW-based generalized measurement is the application of site-dependent coin rotations to control the coin's internal dynamics and, thereby, effect the evolution of the walker. Thus, we have demonstrated a new and versatile approach to generalized qubit measurements via photonic quantum walks.

We would like to thank P. Kurzyński, C. F. Li, and Y. S. Zhang for stimulating discussions. This work has been supported by NSFC under Grants No. 11174052 and No. 11474049, the Open Fund from the State Key Laboratory of Precision Spectroscopy of East China Normal University, the CAST Innovation fund, NSERC, AITF, and the China 1000 Talents program.

*gnep.eux@gmail.com

[1] J. Kempe, Contemp. Phys. **44**, 307 (2003).
[2] S. E. Venegas-Andraca, Quantum Inf. Process. **11**, 1015 (2012).
[3] P. Kurzyński and A. Wójcik, Phys. Rev. Lett. **110**, 200404 (2013).
[4] A. M. Childs, Phys. Rev. Lett. **102**, 180501 (2009).
[5] A. M. Childs, D. Gosset, and Z. Webb, Science **339**, 791 (2013).
[6] N. B. Lovett, S. Cooper, M. Everitt, M. Trevers, and V. Kendon, Phys. Rev. A **81**, 042330 (2010).
[7] A. C. Oliveira, R. Portugal, and R. Donangelo, Phys. Rev. A **74**, 012312 (2006).
[8] S. Hoyer, M. Sarovar, and K. B. Whaley, New J. Phys. **12**, 065041 (2010).
[9] M. A. Nielsen and I. L. Chuang, *Quantum Computation and Quantum Information*, Cambridge Series on Information and the Natural Sciences (Cambridge University Press, Cambridge, England, 2000).
[10] J. B. Altepeter, E. R. Jeffrey, and P. G. Kwiat, in *Advances In Atomic, Molecular, and Optical Physics*, edited by P. R. Berman and C. C. Lin, Advances In Atomic, Molecular, and Optical Physics, Vol. 52 (Academic Press, New York, 2005), pp. 105–159.
[11] V. Scarani, S. Iblisdir, N. Gisin, and A. Acín, Rev. Mod. Phys. **77**, 1225 (2005).
[12] C. H. Bennett, G. Brassard, S. Popescu, B. Schumacher, J. A. Smolin, and W. K. Wootters, Phys. Rev. Lett. **76**, 722 (1996).
[13] N. Gisin, G. Ribordy, W. Tittel, and H. Zbinden, Rev. Mod. Phys. **74**, 145 (2002).
[14] B. Huttner, A. Muller, J. D. Gautier, H. Zbinden, and N. Gisin, Phys. Rev. A **54**, 3783 (1996).
[15] R. B. M. Clarke, A. Chefles, S. M. Barnett, and E. Riis, Phys. Rev. A **63**, 040305 (2001).
[16] M. Mohseni, A. M. Steinberg, and J. A. Bergou, Phys. Rev. Lett. **93**, 200403 (2004).
[17] P. J. Mosley, S. Croke, I. A. Walmsley, and S. M. Barnett, Phys. Rev. Lett. **97**, 193601 (2006).
[18] I. D. Ivanovic, Phys. Lett. A **123**, 257 (1987).
[19] D. Dieks, Phys. Lett. A **126**, 303 (1988).
[20] A. Peres, Phys. Lett. A **128**, 19 (1988).
[21] G. M. D'Ariano, M. F. Sacchi, and J. Kahn, Phys. Rev. A **72**, 032310 (2005).
[22] G. Zauner, PhD thesis, University of Vienna, 1999.
[23] G. Zauner, Int. J. Quantum. Inform. **09**, 445 (2011).
[24] J. M. Renes, R. Blume-Kohout, A. J. Scott, and C. M. Caves, J. Math. Phys. (N.Y.) **45**, 2171 (2004).
[25] A. J. Scott and M. Grassl, J. Math. Phys. (N.Y.) **51**, 042203 (2010).
[26] M. A. Broome, A. Fedrizzi, B. P. Lanyon, I. Kassal, A. Aspuru-Guzik, and A. G. White, Phys. Rev. Lett. **104**, 153602 (2010).
[27] T. Kitagawa, M. A. Broome, A. Fedrizzi, M. S. Rudner, E. Berg, I. Kassal, A. Aspuru-Guzik, E. Demler, and A. G. White, Nat. Commun. **3**, 882 (2012).
[28] See Supplemental Material at http://link.aps.org/supplemental/10.1103/PhysRevLett.114.203602 for fidelity of the reconstructed density matrix.